JOURNAL OF
EMERGING
INVESTIGATORS

VOLUME 2, ISSUE 7 | JULY 2019
emerginginvestigators.org

Controlling the Invasion

The potential of different materials for reducing zebra mussel attachment

Cilia mechanics

Investigating how voltage changes affect unicellular organisms

Yeast and asthma

An abundant yeast species may aggravate asthma symptoms

JOURNAL OF EMERGING INVESTIGATORS

The Journal of Emerging Investigators is an open-access journal that publishes original research in the biological and physical sciences that is written by middle and high school students. JEI provides students, under the guidance of a teacher or advisor, the opportunity to submit and gain feedback on original research and to publish their findings in a peer-reviewed scientific journal. Because grade-school students often lack access to formal research institutions, we expect that the work submitted by students may come from classroom-based projects, science fair projects, or other forms of mentor-supervised research.

JEI is a non-profit group run and operated by graduate students, postdoctoral fellows, and professors across the United States.

FOUNDING SPONSORS

Contents

VOLUME 2, ISSUE 7 | JULY 2019

JOURNAL OF
EMERGING INVESTIGATORS

Article

Assessing Materials' Short-term Effectiveness on Controlling Zebra Mussel (*Dreissena polymorpha*) Attachment

Justin Willson and Ann Lambert
King Philip Regional High School, Wrentham, Massachusetts

SUMMARY

Zebra mussels, an aquatic invasive species, cost millions of dollars each year to control due to their extensive attachment on essential industrial structures and detrimental effects on the native ecosystem. Reducing mussel attachment would allow researchers to control what surfaces these mussels attach to, and this reduction would prevent dangerous situations in industrial piping that occur when mussels prevent water flow. The goal of this research was to identify nontoxic materials that were effective in preventing or reducing the strength of zebra mussel attachment. We tested two materials, Sharklet and Netminder, that were designed to prevent biofouling of aquatic organisms, as well as two control materials, PVC pipes and a lake rock. The first experiment determined that Sharklet cannot prevent adult mussel attachment, but there was a statistically significant difference in attachment strength between Sharklet, the uncovered PVC pipe, and the rock. The second experiment determined that Netminder likewise cannot prevent adult mussel attachment and does not have a statistically significant difference in attachment strength with an uncoated PVC pipe. Since the Sharklet demonstrated some ability to deter mussel attachment, the material, along with other micro-engineered surfaces, warrant further study. Netminder likewise requires future study to determine its effect on zebra mussel veligers in a natural environment.

INTRODUCTION

Invasive species are a diverse group of organisms that have been transported to a location that is not in their native range. These organisms are usually extremely well adapted to these new environments; consequently, they spread rapidly with little hope of eradication (1). One of the most prominent aquatic invasive species in the United States is the zebra mussel *Dreissena polymorpha*. Zebra mussels are freshwater mussels that inhabit lakes, streams, rivers, and reservoirs where they attach to stable substrates which often include manmade materials, other animals such as crayfish, and even other zebra mussels (2). Zebra mussels live 3–9 years and have a shell length of 36–46 millimeters (2, 3). These mussels are native to the Black, Caspian, and Azov Seas in eastern Europe but became invasive in 1986 when they were introduced to the Great Lakes after being transported through the ballast water of ships (3, 4). Zebra mussels are now widespread in the United States and are currently found in locations ranging from the Great Lakes Region and the Mississippi River to Laurel Lake in western Massachusetts where they were discovered in July 2009 (5, 6).

Once zebra mussels become established in ecosystems in which they are not native, their superior adaptations in filtration and breeding allow them to thrive at the expense of native shellfish and other organisms. Zebra mussels are prolific breeders; a female produces up to a million eggs each year, and once fertilized, microscopic larvae known as veligers develop and are planktonic for three to four weeks before settling on a suitable substrate (2). This planktonic stage allows for widespread colonization of zebra mussel larvae and rapid spread within and between water bodies. Adult mussels are able to detach and drift short distances to find a more suitable substrate and can spread over land by adhering to boats (2, 3). Zebra mussels commonly reach densities of over 200,000 mussels per square meter and can filter around one liter of water per day (2, 3). As a result of dense zebra mussel colonization, native microorganisms, shellfish, and fish, both adults and larvae, are severely disrupted (2).

In addition to having a profound impact on natural ecosystems, zebra mussels significantly impact industrial operations. Zebra mussels readily adhere to materials such as concrete, carbon steel, and stainless steel, which are common construction materials (3). The strength of attachment varies depending on the substrate, although it generally increases with surface roughness due to increased penetration of the adhesive layer (3). As a result, the mussels often colonize water supply pipes of hydroelectrical and nuclear power plants, public water supply plants, and other industrial facilities in a process known as biofouling (2). This biofouling causes numerous problems that include restricted water flow and intake, decaying organisms in the water, corroding metal and concrete, and reduced flow of cooling water to electric power plants due to pipe blockage (2, 7). Such blockages, corrosion, equipment failures, and possible lake closures are expensive for these facilities and cost millions of dollars per year (7).

Zebra mussels attach to substrates by byssal thread formation, which generally increases with the size of the mussel (3). The byssal threads contain plaques, threads,

stems, and roots (8). The adhesive plaques attach to the substrate in a continuous layer that is electron dense and around 10–20 nanometers thick (8). Threads attach to the individual plaques and the stem holds these threads in a bundle (8). The root is attached to the bundle of threads (8; **Figure 1**). Like many marine mussels, zebra mussels are thought to utilize 3,4-dihydroxyphenylaline (DOPA), an uncommon amino acid, to adhere to substrates (8). The distinct composition of the adhesive layer and the spatial distribution of proteins within it are unknown, which limits the understanding of the adhesion process (8). It is understood, however, that mussels use DOPA-mediated bidentate hydrogen bonding to attach to a wide variety of surfaces, which is double the strength of a normal hydrogen bond, metal/metal oxide coordination, or oxidative cross linking (9). Mussels can form bidentate hydrogen bonding when the material has hydrogen bonding sites. Coatings that contain epoxy, urethane, and urea linkages are susceptible to this type of bonding (9).

Figure 1: Byssal threads. An image of zebra mussel threads when a mussel was being removed from a lake rock at Laurel Lake.

Researchers have been attempting to create a surface or coating that prevents biofouling; however, there is currently no product that is fully capable of preventing biofouling while remaining both safe for the environment and durable. Some methods, such as copper-based heavy metal coatings, are effective and durable but hazardous to the environment (3, 5). Antifouling paints also commonly contain biocides such as copper and only last 1–2 years in flowing water (5). Other foul release coatings, such as silicone, are nontoxic but are also susceptible to abrasion and eventual depletion (3).

The goal of this research was to identify coatings or materials that are durable, environmentally friendly, and could be used to control zebra mussel adherence on industrial surfaces such as pipes. We tested Sharklet, a micro-engineered surface, and Netminder, a self-polishing water-based release coating. These materials were chosen primarily due to their availability, but also due to their nontoxic properties, which separate them from heavy metal coatings and antifouling paints.

Sharklet is a micro-engineered material with an embedded primary surface pattern that is diamond shaped with rows 3 microns tall and 2 microns wide. The pattern and dimensions can be modified depending on the application and the pattern can either protrude outward from the surface or be recessed into the surface (11). This pattern is based on shark skin, which naturally prevents biofouling in a marine environment (11). Sharklet is part of a group of materials known as micro-engineered surfaces. These materials can be based on surfaces in nature and improve performances of foul release coatings, but the optimal size of the surface pattern is different among organisms (3). Thus, the width and spacing of topographical patterns may need to be tailored to specific organisms (10).

Netminder is a water-based and self-polishing silicone release coating that is marketed as a nontoxic alternative to copper, zinc, or organotin based products (12). This coating is photoactive and requires an illuminated environment to work properly (12). When in oxygenated water, Netminder generates low levels of peroxides at its surface that are said to control the settlement of larvae and adults of marine biofouling organisms (12). The peroxides then dissociate into water and oxygen, making the coating nontoxic (12). Netminder most closely resembles a foul release coating, specifically a silicone foul release coating. This type of antifouling coating works either by slowly eroding and removing biofouling or minimizing attachment strength due to the unique chemical properties of the coating (3). These coatings are generally considered safe for the environment because they do not use biocides; however, some materials in the paint itself such as zinc are considered toxic (3). Silicone based foul release coatings are generally considered the best performing foul release coatings due to their low elastic modulus that releases organisms by peeling instead of shearing (9). Some silicone foul release coatings can prevent mussel attachment, and these coatings are generally considered nontoxic compared to antifouling paints but are susceptible to abrasion. In addition, these coatings sometimes get fouled with algae and aquatic vegetation, which then leads to zebra mussel attachment (3). Increased water flow can further decrease the lifespan of biocide based foul release and antifouling coatings (3).

We hypothesized that due to their unique properties as micro-engineered surfaces or water-based release coatings, Sharklet and Netminder would negatively affect the strength of zebra mussel attachment when compared to a common industrial piping surface (PVC).

RESULTS

This study tested the short-term effectiveness of two materials, Sharklet and Netminder, on preventing adult zebra mussel attachment in a laboratory setting. The research was divided into two experiments: Experiment 1 compared Sharklet to control surfaces, and Experiment 2 compared Netminder to a control surface, with each experiment being divided into two trials. It is important to note that each experiment has its own control because Experiment 1 began in May and Experiment 2 began in August and each used a different set of mussels. In all trials, some mussels did not attach to the target material; therefore, the data from Trials 1A and 1B were combined in the reported results of Experiment 1 and the data from Trials 2A and 2B were combined in the reported results of Experiment 2.

In Experiment 1, we tested the mussel attachment on the Sharklet covered PVC compared to a rock and an uncovered PVC pipe in two trials, Trial 1A and Trial 1B. Over two trials, 12 mussels attached to the rock out of 20 total mussels (60.0%). Out of 40 total mussels, 17 mussels attached to the uncovered PVC pipe (42.5%). For the Sharklet covered PVC pipe, 12 mussels attached out of 40 total mussels (30.0%; **Figure 2**). Mussels that were not found on the target material were either attached to the glass, other mussels, rocks holding the PVC pipe down, or had become inactive or dead. This occurrence happened in both trials of the experiment. Experiment 1 also compared the mussel attachment strengths to the rock, PVC pipe, and Sharklet (**Figure 3**). On the rock, the mean attachment strength was 0.82 pounds, the median attachment strength was 0.74 pounds, and the standard deviation was 0.39 pounds. On the uncovered PVC, the mean attachment strength was 0.63 pounds, the median attachment strength was 0.59 pounds, and the standard deviation was 0.39 pounds. On the Sharklet covered PVC, the mean attachment strength was 0.37 pounds, the median attachment strength was 0.32 pounds, and the standard deviation was 0.24 pounds. The attachment strength data in Experiment 1 tended to be skewed right possibly due to attachment strength having a natural limit of zero and the presence of a high outlier in the Sharklet group. This asymmetry happened with most data sets except for the rock (**Figure 3**), indicating that in a natural environment zebra mussel population attachment strength could be normally distributed. A one-way ANOVA test was used to test for a statistical significance in the measured attachment strengths of the three different surfaces with the significance level set at 0.05. The *p*-value of the test was 0.012, indicating that there is a statistically significant difference in the mussel attachment strengths on the three surfaces.

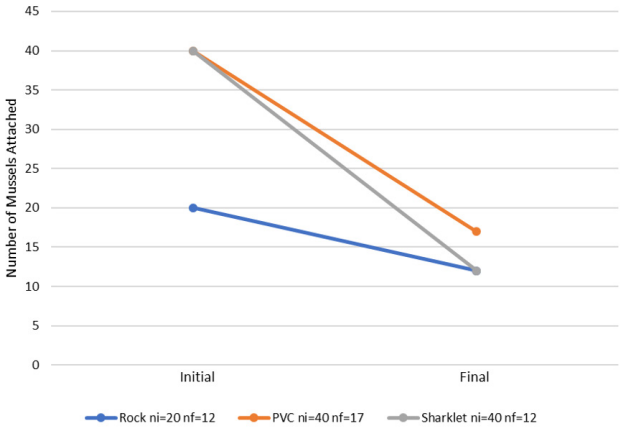

Figure 2: Mussel attachment rates in Experiment 1. The rock (blue), PVC (orange), and Sharklet (gray) mussel attachment rates are shown. The initial point represents the total original number of mussels placed on the material (ni) and the final point represents the total number of mussels that were attached at the conclusion of the trials (nf).

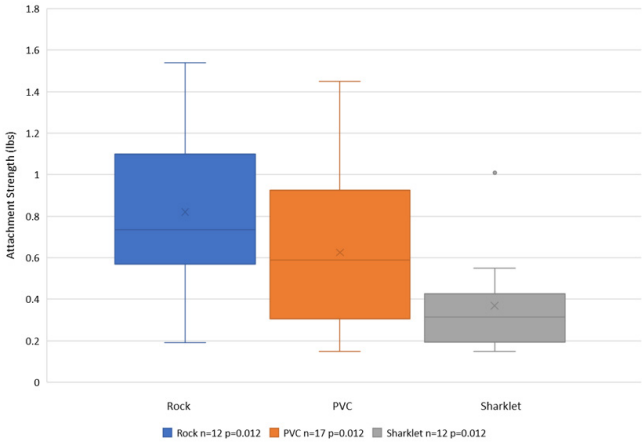

Figure 3: Comparing the distributions of attachment strength in Experiment 1. The distributions of mussel attachment strength values are displayed with the number of mussels (n) and the p value of the ANOVA test (p) displayed below each labeled material. The line in the middle of the box represents the median attachment strength, the x in the box denotes the mean attachment strength, and any dots outside the box and whiskers represent outliers.

Experiment 2 tested PVC pipe coated with Netminder against uncoated PVC pipe. Out of 60 total mussels, 27 total mussels attached to the uncoated sections of the PVC pipes (45.0%) and 28 total mussels attached to the Netminder coated sections of the PVC pipes (46.7%; **Figure 4**). On the uncovered PVC, the mean attachment strength was 0.24 pounds, the median attachment strength was 0.19 pounds, and the standard deviation was 0.13 pounds. On the Netminder covered PVC, the mean attachment strength was 0.32 pounds, the median attachment strength was 0.24 pounds, and the standard deviation was 0.23 pounds (**Figure 5**). Similar to Experiment 1, the attachment strength data in Experiment 2 tended to be skewed right possibly due to attachment strength having a natural limit of zero and the presence of two high outliers on both the Netminder and PVC. Using the assumption that zebra mussel attachment strength in the wild could be normally distributed due to the earlier results from the rock, a two-sample *t* test was conducted. The two-sample *t* test tested for a statistical significance in

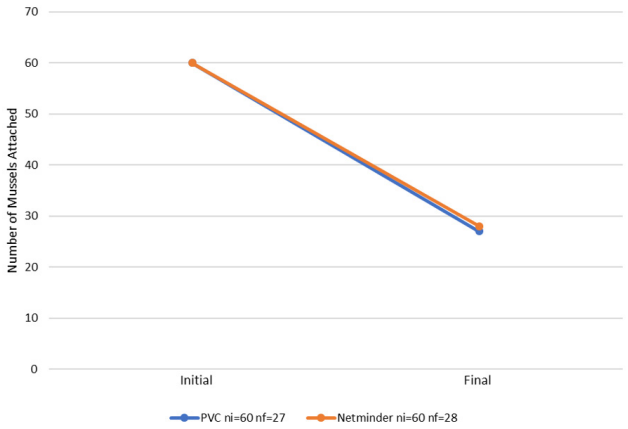

Figure 4: Mussel attachment rates in Experiment 2. The PVC (blue) and Netminder (orange) mussel attachment rates are shown. The initial point represents the total original number of mussels placed on the material (ni) and the final point represents the total number of mussels that were attached at the conclusion of the trials (nf).

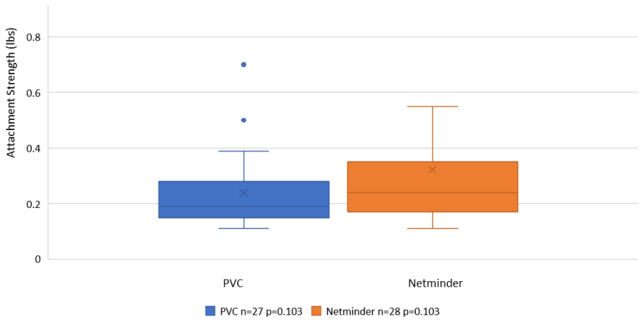

Figure 5: Comparing the distributions of attachment strength in Experiment 2. The distributions of mussel attachment strength values are displayed with the number of mussels (n) and the p value of the two-sample t test (p) displayed below each labeled material. The line in the middle of the box represents the median attachment strength, the x in the box denotes the mean attachment strength, and any dots outside the box and whiskers represent outliers.

the mussel attachment strengths to the Netminder and the uncoated PVC pipe, with the significance level set at 0.05. The *p*-value of this test was 0.103, indicating that there is no statistically significant difference in the attachment strengths of mussels on Netminder coated PVC and uncoated PVC.

DISCUSSION

Zebra mussels were able to attach with varying strength to all materials used during this study. We did not expect that any one material would be able to completely prevent mussel attachment; however, we hypothesized that Sharklet's unique properties as a micro-engineered surface would negatively affect zebra mussel attachment. The results of Experiment 1 suggest that Sharklet does lower the attachment strength of zebra mussels compared to their natural environment and a common industrial material, as it had lower average attachment strengths and there was a statistically significant difference in attachment strengths among those three surfaces. While Sharklet did have the lowest mean and median attachment strengths, it cannot be determined that it was the surface that caused the statistical significance. In Experiment 1, the mussels occasionally moved off the target material to other materials in the tank including the glass, various rocks, and often other mussels. Although the mussel attachment rate on Sharklet was lower, it was not significantly different from the mussel attachment rate on PVC; therefore, it could not be determined which of the two materials the mussels preferred. It is unknown whether Sharklet has been previously tested on zebra mussel attachment strength, as zebra mussel attachment values could not be found in any literature researched, and it is mainly marketed as a method to control the settlement of microorganisms and not freshwater mollusks.

While not able to prevent mussel attachment, Sharklet could still be a promising material for future research. Sharklet demonstrates that its micro-engineered pattern causes lower attachment strength when compared to manmade and natural materials. Although this particular pattern does not prevent attachment in adult mussels, it might be useful for reducing or preventing the settlement of veligers, the microscopic larvae of zebra mussels that are one of their main avenues of colonizing new surfaces. Sharklet's pattern is primarily designed to prevent the colonization of bacteria and other microscopic organisms and has been shown to significantly decrease the settlement of *Ulva*, which are 5 micrometers, and *S. aureus*, which are 0.6 micrometers (10). Since zebra mussel veligers have shell lengths of 70–350 micrometers (3), they could interact with the Sharklet topographical pattern in a similar way to other microorganisms during their initial attachment attempt. The adhesive plaques on adult mussels' byssal threads are one millimeter wide (8) and may be too large to interact with the Sharklet pattern. This hypothesis could be feasibly tested by verifying the presence of veligers in a body of water as well as determining if juvenile mussels attach on the Sharklet material over time. Other micro-engineered patterns might also work better with adult mussels. For example, researchers have developed a mushroom-shaped micro-engineered surface that controls marine barnacle attachment (13), indicating that an ideal pattern may be different between organisms and there is possibly an ideal pattern for zebra mussels.

Similarly, we hypothesized that Netminder's properties as a water-based foul release coating would negatively impact the strength of mussel attachment. Due to the fact that zebra mussels attached to Netminder with similar strength to uncoated PVC, this hypothesis was not supported in the experiment. Experiment 2 suggests that byssal thread formation and attachment among adult zebra mussels is unaffected by the release of peroxides by Netminder in the illuminated environment on a short-term basis. Similar to Experiment 1, mussels did not attach to the desired surfaces for multiple reasons, including being unresponsive or attached to other surfaces that included the glass, rocks, or other mussels. Since zebra mussels attached to both

the Netminder and the uncoated PVC at almost equal rates (46.7% and 45.0% respectively), they did not prefer to attach to either material.

It is also unknown whether Netminder has been tested on zebra mussels before, as no attachment strength values could be found in the literature. In one study conducted by the U.S. Bureau of Reclamation, silicone-based release coatings tested had a maximum attachment strength of 0.40 pounds (5), although these values are hard to compare as the measurement procedure was conducted using a different instrument and the mussels were allowed to attach for a longer period of time in a natural environment. Future research therefore also needs to be conducted on Netminder. The use of peroxides, which dissociate into oxygen and water, is safer for the environment than traditional biocides such as copper. Hydrogen peroxide is also known to control zebra mussel adults and veligers in high doses (7). Although Netminder readily allowed adult zebra mussel attachment, veliger interactions with Netminder's surface would be more prominent in a natural environment; therefore, controlling veliger interactions may be more important in controlling overall mussel attachment. A similar long-term experiment in the natural environment of the mussels as proposed for Sharklet could further determine Netminder's ability to control zebra mussel veliger attachment.

Throughout both experiments, byssal threads were frequently seen on all materials after the attachment strengths were measured and the mussels removed, with the adhesive plaques present on the material and threads still attached to them. Particularly, remaining byssal threads were present on both sides of the Sharklet sheets, indicating that neither side was more effective than the other. The presence of byssal threads demonstrates that for some of the mussels, the attachment strength was only a measure of how strong the threads were; and the actual attachment strength (strength of adhesive plaque to surface attachment) would be a higher value. Another interesting observation to note is the difference in attachment strength values between Experiment 1 and Experiment 2, particularly with respect to unaltered PVC, which was the only common material used in both experiments. In Experiment 1, the PVC had a mean attachment strength of 0.63 pounds while in Experiment 2 its mean attachment strength was 0.24 pounds. It is important to note that this difference could potentially be due to the fact that the mussels were collected at different time of the year. The difference in mussel attachment strengths depending on the time of year suggests that Laurel Lake's conditions change throughout the summer and ultimately impact the zebra mussel population's ability to attach effectively. This difference is not expected to impact results because within the individual experiments the sets of mussels used were collected from the lake at the same time. Overall, while both Sharklet and Netminder were hypothesized to decrease mussel attachment strength, there was only evidence that there was a significant difference in attachment strength between Sharklet and the two control materials tested against it. Both materials warrant future research, however, due to their unknown effect in a more natural environment and on zebra mussel veligers and juveniles.

MATERIALS AND METHODS

This study researched the effect of two materials, Sharklet and Netminder, on preventing or reducing the strength of adult zebra mussel attachment in a laboratory setting. Zebra mussels were obtained on two occasions from Laurel Lake at the boat launch shoreline in Lee, Massachusetts. Zebra mussels were obtained with the permission of Jim Straub of the Massachusetts Department of Conservation and Recreation who also advised the disposal of water and mussels after the experiment was completed. Fifty mussels were collected for Experiment 1 in May 2018 and 61 Mussels were collected for Experiment 2 in August 2018. All mussels were collected by removal from shoreline rocks by hand in shallow water under supervision. Waders were worn to minimize contact with the lake water that contains zebra mussel veligers. Zebra mussels were transported from Laurel Lake to the laboratory in a bait bucket, a small circular container with a removable top. The mussels remained in this bait bucket with aeration for three to four hours until the experiments were set up, at which time they were moved into the aquarium. For both experiments, approximately 20 gallons of lake water were taken and used to house the mussels. A flat rock on the shoreline was also taken during the first collection to provide a control surface during Experiment 1 and to hold a PVC pipe underwater during Experiment 2.

Zebra mussels were contained in an Aqueon brand 20-gallon fish tank (30.25" x 12.50" x 12.75") for the duration of both experiments with no filtration. The aquarium received aeration from an air pump that fed air through plastic tubing to two air stones, which released air into the water that could be controlled by valves. In Experiment 1, the tank was covered by a plastic bin cover; however, a light was needed in Experiment 2, so a cover was not used. In Trial 1A, powdered *Chlorella* algae was fed to the mussels; however, this method polluted the tank water so live *Chlorella* algae was bought and cultured for the remaining trials. Once the culture was sustainable, live *Chlorella* algae was fed to the mussels daily. This method was used in Trials 1B, 2A, and 2B of experimentation.

Experiment 1

Experiment 1 tested the effectiveness of Sharklet in preventing short-term adult zebra mussel attachment and incorporated the combined data from Trials 1A and 1B. The Sharklet was cut into multiple small sheets. The Sharklet pattern was confirmed by shining a laser through the sheets, which made a distinct light arrangement due to the surface pattern (**Figure 6**). Three-inch diameter PVC pipes were used in both experiments as control substrates since they have been extensively tested and zebra mussels are known to attach to them with intermediate strength (14, 15). The PVC pipes were

bought from a local vendor and cut into 20-inch segments. The pipes were cut in half so that the top of the pipe would be open, and the zebra mussels could be accessed to measure attachment strength. In both experiments, rocks were put on top of the PVC pipes to hold them down at the bottom of the aquarium since they float. This setup still allowed the mussels to have full access to the entire surface of the pipes (**Figure 7**).

Trial 1A was set up with two PVC pipes, one covered with Sharklet and one without it, and the flat rock from Laurel Lake. The PVC pipe with Sharklet was covered by eight sheets of Sharklet, four of which were approximately 4.5" x 2.25" and

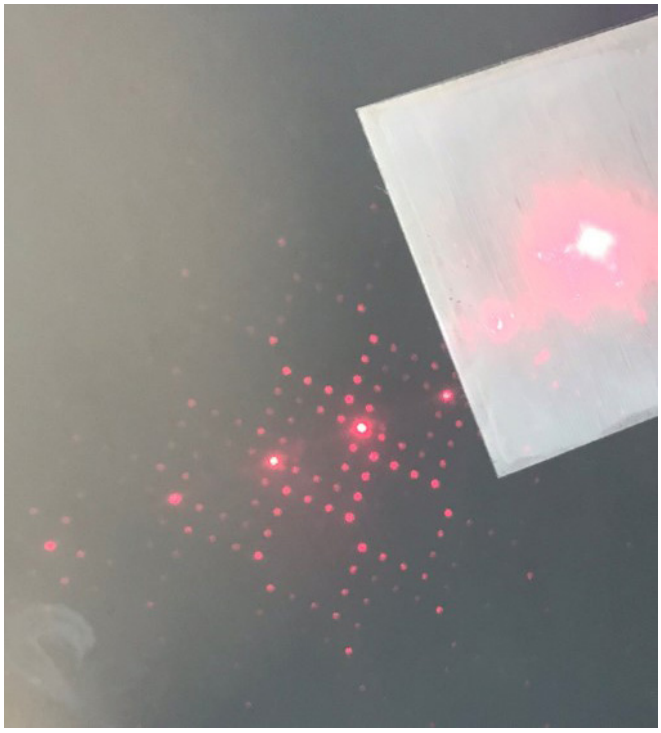

Figure 6: Sharklet Laser Pattern. This original image displays the distinct light pattern created by Sharklet's micro-engineered surface when a laser is shined through it.

the remaining four were approximately 3.0" x 2.0." Both PVC pipes and the rock were separated by a plastic mesh tank divider that was anchored to the walls of the aquarium using suction cups. 20 mussels were placed on the Sharklet covered PVC pipe, 20 mussels were placed on the uncovered PVC pipe, and 10 mussels were placed on the lake rock. A smaller number of mussels was placed on the rock due to its small surface area. The mussels were placed by hand and evenly spaced along the length of the covered and uncovered PVC pipes and the rock. The lake rock was used as a control to make sure mussels would behave in the same way as in Laurel Lake. Ten days after the day of placement, the attachment strength of the zebra mussels was measured. The measurements were taken in pounds using a Quarrow Fish Lip Grip Digital Fishing Scale (50-pound capacity) and

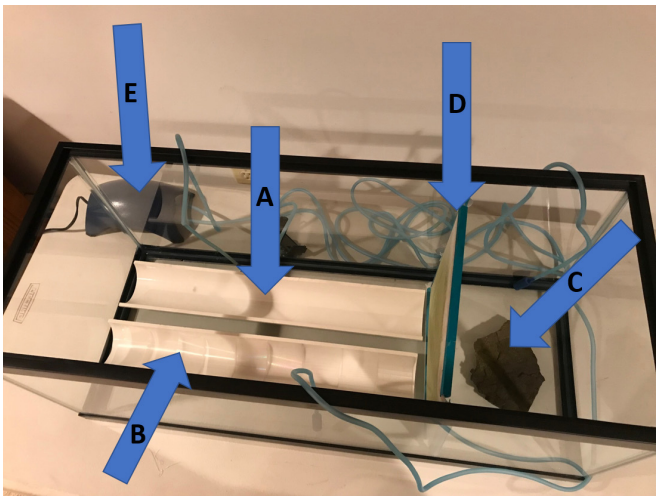

Figure 7: Experiment 1 Design. This original image displays all components of the design of Experiment 1: (A) the uncovered PVC, (B) Sharklet covered PVC, (C) lake rock, (D) tank divider, and (E) aeration system.

the data was recorded. The scale usually measures a pulling force, but it was not practical to attach the stainless-steel jaws to a mussel and pull it off a surface. Instead, the pushing force was measured since the scale can read pushing forces as negative numbers. The negative sign was ignored for the experiment. A Magic Sliders brand felt pad was cut into a half circle and glued onto the end of the steel jaws to prevent shell breakage and provide a greater surface area for measurement. When measuring attachment strength, the scale was first zeroed, and then light pressure was applied against the mussel's shell by pushing the felt pad against the shell. Increasing force was applied to the mussel's shell until the mussel became dislodged from the surface it was attached to. The highest reading before the mussel became dislodged was taken as the attachment strength. If an individual mussel was attached to a surface and had other mussels attached to it, this was known as a cluster. If the mussels attached could be removed, the individual's attachment strength was measured; however, this was inconsistent as sometimes the arrangement of the cluster did not allow for removal or all mussels became dislodged with the removal of one mussel. Since the mussels could move freely throughout the PVC area and the glass bottom and sides of the aquarium, the number of mussels on each surface were recorded as well. The same procedures for measuring attachment strength for individuals, clusters of mussels, and counting the number of mussels on each surface were followed in both experiments. The PVC pipes and Sharklet sheets were cleaned of any waste, algae, or other debris before the next trial began.

Trial 1B was set up in the same way as Trial 1A, with 20 mussels on the uncovered PVC pipe, 20 mussels on the PVC pipe with Sharklet and 10 mussels on the lake rock and all components in the same positions. The mussels on each section were not necessarily the same mussels from Trial 1A as they were picked randomly during placement. The only

difference in the setup was in the placement of the Sharklet. The four small sheets of Sharklet became dislodged from the PVC pipe in Trial 1A so they were not used in Trial 1B. Since no more large sheets were available, the four large sheets were placed together on one side of the pipe and all mussels were placed on these sheets. To achieve similar spacing on the uncovered pipe, the mussels on that pipe were also hand placed in the same corresponding area of the pipe. Ten total days after placement, the attachment strength was measured and recorded using the same procedure as Trial 1A. In both trials, some zebra mussels moved off the target material, were unresponsive, or attached to themselves to form clusters. These numbers were included in the analysis of the attachment rates of mussels but decreased the number of data points to analyze for attachment strength. Therefore, the data from Trials 1A and 1B were combined in the reported results of Experiment 1.

Experiment 2

Experiment 2 tested the effectiveness of Netminder at preventing short-term adult zebra mussel attachment. Experiment 2 was also divided into two trials, Trial 2A and Trial 2B, with each trial again lasting 10 days. Thirty mussels were placed on each material. Sixty total mussels were placed on both the PVC pipe and the Netminder during this experiment. A one-quart sample of Netminder was generously provided by Alex Walsh, the Director of Research and Product Development of ePaint. Since Netminder is photoactive, a Coralife 6700K 96-watt light was used in both Trial 2A and Trial 2B. The right end of the light rested on one five-gallon bucket while the left end of the light rested on the right edge of the aquarium and was suspended nearly halfway across the right side of the aquarium. In between the right side of the aquarium and the five-gallon bucket was the *Chlorella* algae culture that also needed the light to continue growing. The light provided lighting to the whole aquarium, but the right side received stronger light than the left. The light ran on a 12-hour timer to ensure that the same amount of light was received during each trial. Netminder was applied by brush to the right half of three new PVC pipes that were cut in the same way as those from Experiment 1. One coat was applied by brush under supervision following the package instructions. 3M Nitrile gloves, goggles, and a mask were worn to protect from the paint and fumes.

Trial 2A was set up with the three PVC pipes secured by rocks, including one lake rock from Experiment 1. The pipes were arranged so that they aligned horizontally. The Netminder-coated half of the pipes were oriented into the stronger light (**Figure 8**). On each PVC pipe, 10 mussels were hand placed on the coated half and 10 mussels were placed on the uncoated half. In total, 30 mussels were on the Netminder coated sections of the PVC pipes and 30 mussels were on the uncoated sections. The remaining mussel was placed on the glass away from the PVC pipes. Mussels could move freely between the two halves of the PVC pipes. After 10 days of placement in the tank, the attachment strength of the zebra mussels was measured using the same procedure, the data was recorded, and the pipes were cleaned.

Trial 2B was set up in the same way as Trial 2A. A total of 30 mussels were hand placed on the Netminder coated section of the PVC pipes and 30 total mussels were placed on the uncoated sections. On each pipe, 10 mussels were hand placed on each section. One mussel from Trial 2A died (its shell was open and would not close); therefore, that mussel was replaced with the extra that was placed on the glass in Trial 2A. The mussels were picked randomly when placed so the same individuals were not necessarily in the same places as Trial 2A. The light was raised approximately 1.5 feet due to concerns that intense light was causing increased mussel mortality; however, 7 total mussels died on the uncoated PVC and 9 total mussels died on the Netminder coated PVC by the conclusion of Experiment 2. The mussel attachment strength was measured by the same procedure as in previous trials. Similar to Experiment 1, the movement of mussels off the target materials and the increased mortality of mussels decreased the number of mussels that could be used to measure attachment strength. As a result, the data from Trial 2A and Trial 2B were combined in the reported data of Experiment 2.

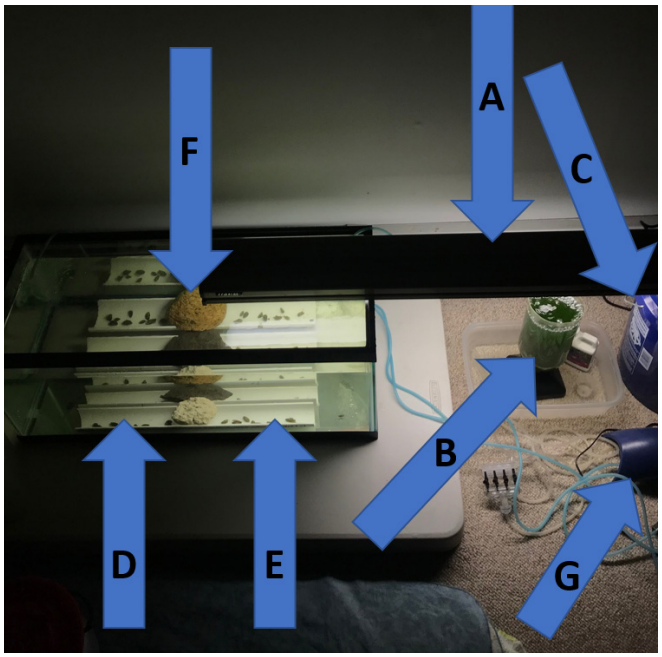

Figure 8: Experiment 2 Design. This original image displays all components of the design of Experiment 2: (A) The light, (B) *Chlorella* algae culture, (C) five-gallon bucket, (D) PVC, (E) Netminder coated PVC, (F) rocks, and (G) aeration system.

Safety Procedures

Throughout both experiments, certain procedures were followed to eliminate the potential spread of zebra mussels or veligers into the water supply or nearby bodies of water.

The aquarium was kept covered during Experiment 1, but this was not possible in Experiment 2. Waterproof gloves were worn when filling the tank with water, handling the mussels or experiment equipment, and measuring mussel attachment strength (except when removing mussels from another mussel individually attached to a surface) to minimize contact with lake water. Gloves were not worn when the mussels were collected from Laurel Lake or placed on the PVC pipes in the aquarium because these tasks required increased accuracy that could not be replicated when the gloves were worn. Occasionally water did make contact with skin or the gloves did not adequately prevent water contact. In these circumstances, hands were not immediately washed as this could spread veligers into the water supply. Instead, hand sanitizer containing 70% Ethyl Alcohol was used to kill potential veligers.

The following disposal procedures were required by Jim Straub to ensure no spread of invasive species. The experiment was conducted away from drains, sinks or other areas that connect to the water supply. After Experiment 1 concluded, all lake water was disposed of in the middle of a grassy yard. The PVC pipes, Sharklet, waders, gloves, scale, rocks, containers, buckets, aquarium, and other materials used were dried inside between the two experiments. The zebra mussels were counted and confirmed as 50, the original number. After confirmation, the mussels were placed in two sealed plastic bags and disposed of in the trash along with other disposable materials that were used during Experiment 1. After Experiment 2 concluded, the number of mussels was confirmed as 61, the same as the original amount; and they were disposed of in the same way as Experiment 1. The aquarium water and extra lake water were again disposed of outside in a yard rather than down a drain. Some materials, including the gloves, air pump tubing, air stones, and the tank divider were disposed of in the trash. Other materials, including the aquarium, towels, five-gallon buckets, and covers were placed inside during rainy days and outside during dry days to dry. These materials were dried outside for a minimum of seven days, not necessarily consecutively, as advised.

ACKNOWLEDGEMENTS

Thank you to Mr. Jim Straub of the Massachusetts Department of Conservation and Recreation for giving permission to collect zebra mussels and advice about disposal; otherwise this project would not be possible. A special thanks goes out to Mr. David W.H. Wong of the Massachusetts Department of Environmental Protection who gave advice about where to collect the mussels and how to obtain permission to do so. Another special thank you goes out to Mr. Alex Walsh, who generously provided a sample of Netminder to test. Thank you to Mr. John Willson for giving crucial advice for the project. A final thank you goes out to Mrs. Doris Brennan who provided the device to grow the algae in and gave advice for the paper and Mr. Chris Rando who cut the PVC pipes.

Received: October 29, 2018
Accepted: January 30, 2019
Published: June 3, 2019

REFERENCES

1. Worden, David. “Aquatic Invasive Species Assessment and Management Plan.” Massachusetts Department of Conservation and Recreation, October 2010, https://www.mass.gov/files/documents/2017/10/10/aquatic.pdf.
2. “State of Michigan’s Status and Strategy for Zebra and Quagga Mussel Management.” State of Michigan, 2014, https://www.michigan.gov/documents/deq/wrd-ais-dreissenids_499881_7.pdf.
3. Sytsma, Mark, and Steven Wells. “A review of the Use of Coatings to Mitigate Biofouling in Freshwater.” Portland State University: Centers for Lakes and Reservoirs, 2009, http://citeseerx.ist.psu.edu/viewdoc/download?doi=10.1.1.458.7807&rep=rep1&type=pdf.
4. Baldwin, Wen, Shawn Gerstenberger, Bryan Moore, and Wai Hing Wong. “Settlement and Growth of Quagga Mussels (*Dreissena rostriformis bugensis* Andrusov, 1897) in Lake Mead, Nevada-Arizona, USA.” *Aquatic Invasions*, vol. 7, no. 1, 2011, pp. 7-19. http://www.aquaticinvasions.net/2012/AI_2012_1_Wong_etal.pdf.
5. “Coatings for Mussel Control-Results from Six Years of Field Testing.” U.S. Bureau of Reclamation, July 2014, https://www.usbr.gov/mussels/docs/MERL2014-64Coatings.pdf.
6. “Zebra Mussel Phase I Assessment: Physical, Chemical, and Biological Evaluation of 20 Lakes and the Housatonic River in Berkshire County, Massachusetts.” Biodrawversity LLC, November 2009, https://www.mass.gov/files/documents/2017/10/10/phase%20i.pdf.
7. Glomski, L.M. “Zebra Mussel Chemical Control Guide Version 2.0.” US Army Engineer Research and Development Center, July 2015, https://erdclibrary.erdc.dren.mil/xmlui/bitstream/handle/11681/6966/ERDC-EL-TR-15-9.pdf?sequence=1&isAllowed=y.
8. Farsad, Nikrooz, and Eli D. Sone. “Zebra Mussel Adhesion: Structure of the Byssal Adhesive Apparatus in the Freshwater Mussel, *Dreissena polymorpha*.” *Journal of Structural Biology*, vol. 177, no. 3, pp. 613-62. doi: 10.1016/j.jsb.2012.01.011.
9. Merten, Bobbi Jo, Allen D. Skaja, and David Tordonato. “Coatings for Invasive Mussel Control: Colorado River Field Study.” *Biology and Management of Invasive Quagga and Zebra Mussels in the Western United States*. 2015, pp. 451-466. doi: 10.1201/b18447-37.
10. Brennan, Anthony B., Scott P. Cooper, and Chelsea M. Magin. “Non-toxic Antifouling Strategies.” *MaterialsToday*, vol. 13, no. 4, 2010, pp. 36-44. *ScienceDirect*. doi: 10.1016/S1369-7021(10)70058-4.
11. Sharklet Technologies, www.sharklet.com.

12. Netminder Aquaculture Coatings, www.netminder.us.
13. Allen, Michael. “Barnacles are no Match for Mushroom-shaped Microstructures.” *PhysicsWorld*, 27 August 2018, physicsworld.com/a/barnacles-are-no-match-for-mushroom-shaped-microstructures/.
14. Gerstenberger, Shawn L., Sara A. Mueting, and Wai Hing Wong. “An Evaluation of Artificial Substrates for Monitoring the Quagga Mussel (Dreissena bugensis) in Lake Mead, Nevada-Arizona.” *Lake and Reservoir Management*, vol. 26, no. 4, 2011, pp. 283-292. doi: 10.180/07438141.2010.540700.
15. Coyle, Benjamin P., Paul H. Lord, and Wai Hing Wong. “Monitoring Zebra Mussel Colonization: PVC and Cast Iron Recruitment.” http://www.oneonta.edu/academics/biofld/PUBS/ANNUAL/2014/14%20Coyle%20Adherence%20Monitoring.pdf.

Financial Support: Thanks to JEI Sponsor Alloy Therapeutics for support of this article’s publication.

JOURNAL OF
EMERGING INVESTIGATORS

Article

Cathodal galvanotaxis: the effect of voltage on the distribution of *Tetrahymena pyriformis* across a capillary tube

Christy Zheng[1], Michael Edgar[1]
[1]Milton Academy, Milton, Massachussets

SUMMARY

***Tetrahymena pyriformis* are unicellular eukaryotes with thousands of hair-like structures called cilia on the surface of their bodies that aid in cell motility and food consumption. The similarities between their cilia and that of humans, particularly in the human respiratory and olfactory track, are why they are model organisms for investigating cell movement and cilia functionality. Further research may help scientists better understand how cilia are affected by common ciliopathies, genetic disorders caused by the abnormal formation or function of cilia. The objective of this experiment was to investigate the effect of voltage on the distribution of *T. pyriformis* across a capillary tube. *T. pyriformis*-filled capillary tubes were connected to a power supply for one minute. We calculated the percent distributions at the anode and cathode of the capillary tube by counting *T. pyriformis* with a hemocytometer. Our results indicate that cathodal galvanotaxis is induced at 4V and that, despite increases in voltage from 4–30V, the percent distribution of *T. pyriformis* at the cathode remained constant at approximately 80%. These data suggest that while calcium and potassium voltage-gated ion channels are mediated by graded potentials and are triggered at specific thresholds, further increasing voltage above that threshold had little effect.**

INTRODUCTION

Galvanotaxis refers to the movement or innate behavioral response of cells toward an electrical stimulus. Cell galvanotaxis, particularly migration patterns and migration speeds, is often investigated and applied to research in cell signaling, tissue regeneration, and microcellular robotics (1). In this experiment, we used *Tetrahymena pyriformis*, a unicellular eukaryote 30–50 µm in size, because supplying voltage through its surrounding conductive media induces quick behavioral responses that can be readily quantified. *T. pyriformis* possess hundreds of cilia—fine, hair-like projections—along their membranes. Studying their function can therefore allow us to gain insight into the ciliary linings found in the respiratory and olfactory tracts of mammals (2, 3). These repeating cilia units are *T. pyriformis*'s defining structures responsible for efficient cell motility (i.e., the independent movement of an organism). The interaction of electrical current with potassium and calcium channels on cilia membranes results in cell movement towards the negative, or cathode, end of an electrolytic cell (4). More specifically, the direction and speed of propulsion are dependent on the influx of potassium and calcium ions into the cell and, in turn, the oscillation of rows of cilia at specific frequencies (5). Thus, galvanotaxis is a simple method used to assay overall cell movement and to better understand cilia functionality. Research in this field may provide insight into cilia functionality and could potentially help treat common ciliopathies, such as Bardet–Biedl syndrome (BBS) and Alström syndrome (ALMS). Both BBS and ALMS are characterized by vision and hearing impairment, which arise due to mutations in proteins implicated in ciliary function (6).

Because cilia are vital to cellular mobility, it should be noted that several factors can cause deciliation (the loss of cilia) in *T. pyriformis*. Specific temperatures, calcium inhibitors, cytoskeleton inhibitors, protein synthesis inhibitors, and various types of media can cause deciliation, rendering *T. pyriformis* immobile and unable to feed themselves. However, the process in which galvanotaxis affects the movement and direction of cilia movement is unlike the process of cell deciliation.

The media solution in which *T. pyriformis* are subcultured is an electrolyte, a conductive medium that allows voltage to be supplied through the solution. When voltage is supplied through the medium, a potential difference between intercellular and extracellular potential is generated across the *T. pyriformis* cellular membrane. A higher voltage is applied and as this potential difference increases, the cell becomes hyperpolarized at the anode, which in turn triggers voltage-gated potassium channels to open and release potassium ions from the cell (**Figure 1**) (5). As a result, the cilia on this side of the *T. pyriformis* beat faster. On the side of *T.*

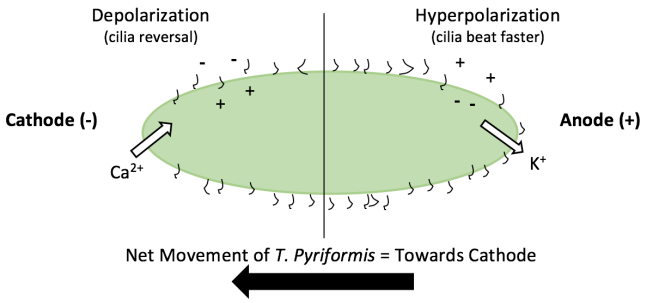

Figure 1. Diagram of the mechanism underlying *T. pyriformis* cathodal galvanotaxis. Depolarization due to influx of calcium ions aligns the cell towards the cathode and hyperpolarization due to outflux of potassium ions in *T. pyriformis* increases cilia beating rate.

pyriformis facing the cathode, depolarization causes voltage-gated calcium channels to open, after which the difference in electrochemical gradient causes calcium ions to flood into the cell. As a result, these cilia beat in reverse. The net effect of depolarization at the cathode and hyperpolarization at the anode results in *T. pyriformis* swimming towards the cathode. If cells are orientated in the opposite direction or perpendicular to the electrical fields, the torque generated from the electrical fields immediately causes the cells to realign themselves to face the cathode (7).

Previous studies have confirmed cathodal galvanotaxis of *T. pyriformis* at 5V, but the extent to which voltage affects cell distribution remains unclear (7). Thus, the goal of this experiment was to determine how increasing voltage would affect the distribution of *T. pyriformis* across a capillary tube, with the distance travelled used as a proxy measurement for the net effect of each subset of cilia beating in a different direction. We hypothesized that because calcium channels affect the direction of cell movement and potassium channels affect the rate at which cilia beat, the ion channels will behave in a graded manner; increasing voltage would increase the magnitude of depolarization and hyperpolarization of ions in the membrane and, thus, increase the distribution of *T. pyriformis* at the cathode end of the tube. Our results reveal that galvanotaxis is induced at 4V and that an increase of voltage beyond 4V yields a distribution of approximately 80% at the cathode.

RESULTS

To determine the effect of voltage on the *T. pyriformis* distribution, *T. pyriformis* were exposed to 0V-30V for one minute. By comparing the cell distribution in the anodes and cathodes of capillary tubes, we determined that increasing the voltage supplied through the *T. pyriformis* solution resulted in galvanotaxis at 4V or greater (**Figure 2**; $p<0.0125$, two-tailed t-test with Bonferroni correction). We also found that the average normalized percentage of cell distribution at the cathode or anode across the different voltages was similar between treatment groups at 0 and 2V, which both show about a 50% distribution of cells at each end of the capillary tube ($p>0.05$, two-tailed t-test). Cell distributions for treatment groups at 10, 20 and 30V were also similar, with roughly 80% of cells localized toward the cathode in each case ($p>0.05$, two-tailed t-test). The distribution of the treatment group at

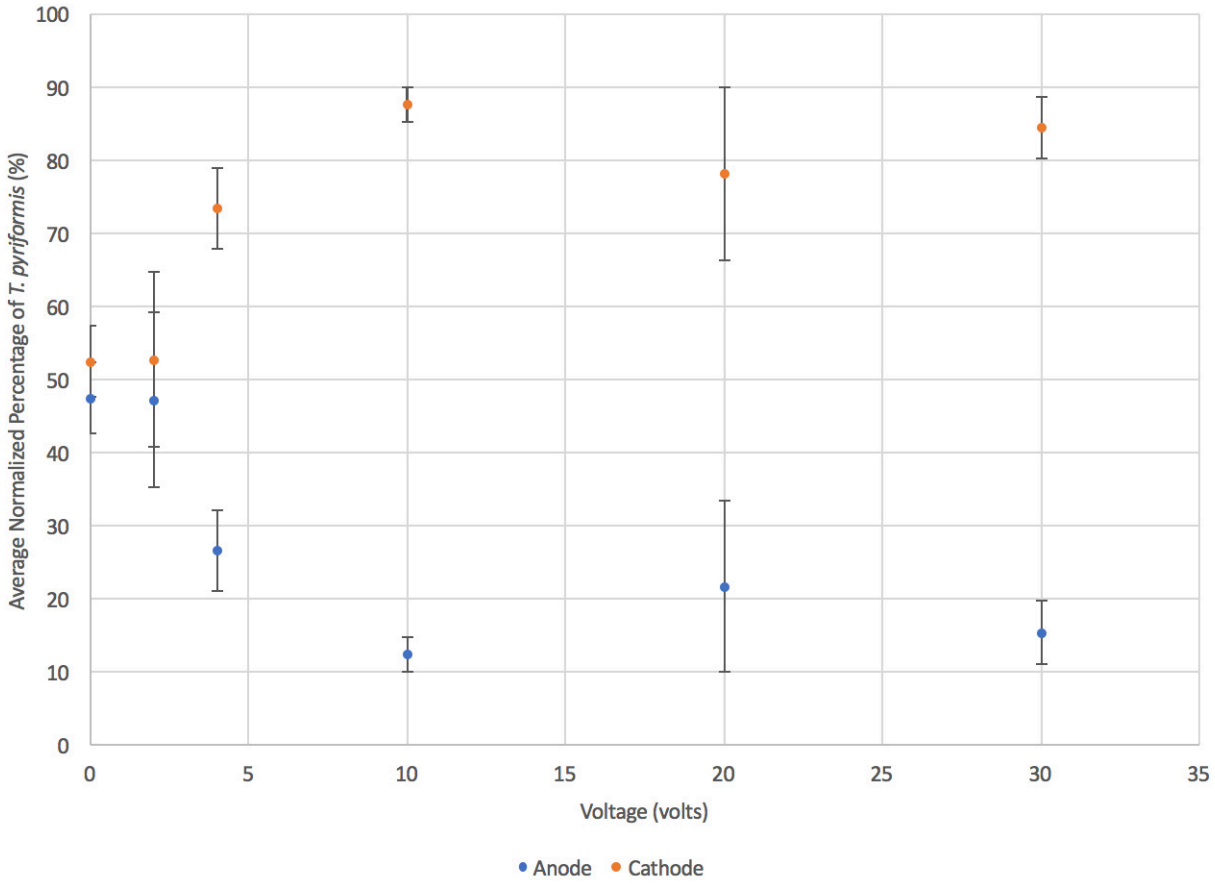

Figure 2. Distribution of *T. pyriformis* in the anode and cathode of the capillary tube at different voltages. The average normalized percentage of *T. pyriformis* in the anode and cathode of the capillary tube when induced to 0-30V for one minute (n=5-6) was plotted. Error bars represent the average absolute deviation value for the five trials at different voltages. The distribution of *T. pyriformis* in the anodes and cathodes was significantly different at 4 to 30 volts ($p<0.0125$, two-tailed t-test with Bonferroni correction). The cell distribution was similar across 0 and 2V ($p = 0.964$) but was significantly different between 0V or 2V and 4, 10, 20 and 30V ($p<0.05$, two tailed t-test).

4V is statistically different from the distribution at 10 and 30V (p<0.05, two-tailed t-test). Thus, our results reveal that galvanotaxis was induced at 4V and that further increases in voltage has little effect on cell distribution.

DISCUSSION

We found that the distribution of *T. pyriformis* at both the anode and the cathode was approximately 50% for groups treated with 0V and 2V. This finding indicates that galvanotaxis only occurs when *T. pyriformis* is exposed to a voltage of 4V or greater. The fact that average normalized percentage of *T. pyriformis* in the cathode was ~50% at 0V and 2V, ~75% at 4V, and ~80 % at 10-30V supports our hypothesis that there is a linear increase in the percentage of *T. pyriformis* that migrate to the cathode as the voltage increased. Closer examination of the data suggests that the average normalized percentage of *T. pyriformis* in the cathode plateaued to 80% during galvanotaxis, supported by the constant percentage of *T. pyriformis* at the cathode despite the wide range of voltage experimented with.

The hypothesis that *T. pyriformis* distribution at the cathode would increase in response to an increase in voltage was based on the concept of graded potentials, where an increase in stimulus results in a greater change in membrane potential (8). When the threshold, or change in membrane potential, for voltage-gated ion channels is met, the channels are open 50% of the time. However, at lower and higher voltages, the decreases and increases in membrane potential affect the amount of time the channels are open as well as the speed at which ions travel through the channels. We speculate that the constant distribution of *T. pyriformis* at the cathode when exposed to 10-30V is because the increase in voltage has no effect on the magnitude of response, and thus biological behavior, that occurs as a result of depolarization in the cell. Voltage-gated ion channels are mediated by graded potentials and are activated at specific thresholds. Consequently, if this threshold is not met, ions will still flow through some channels, but not enough for galvanotaxis to occur (8). Our data suggests that beyond 10V, the same response, or same distribution of cells, occurs. When examined under the microscope, a clear change in swimming movement is observed specifically when voltage is increased from 2 to 4V, demonstrating the point at which enough ions are passing through the channels to cause cathodal galvanotaxis.

Furthermore, the fact that cell distribution for the treatment group at 4V is significantly different from the distribution at 10V and 30V may be indicative of the threshold of voltage-gated potassium channels not being met. The voltage-gated calcium and potassium channels likely have different thresholds, and it may be possible that at 4V, the triggering of voltage-gated calcium channels causes the cells to orient their position towards the cathode. Without the triggering of the voltage-gated potassium channels, it is possible that *T. pyriformis* do not move as quickly towards the cathode since their cilia do not beat quite as fast.

The major source of uncertainty in our experimental approach was the addition of one drop of iodine solution to fix the 25µL of *T. pyriformis* in the anode or cathode. We estimated the volume of one drop to be approximately 50 µL; however, since we did not use a micropipette to be precise in measuring the amount of iodine, there was a large amount of uncertainty in cell counts, especially because of the large volume of iodine added relative to the volume of *T. pyriformis*. This variability likely explains much of the high percent average absolute deviation (AAD) seen in our data and could easily be eliminated with the use of a micropipette to add a smaller volume of iodine.

Another source of uncertainty that may have affected the distribution of *T. pyriformis* across the capillary tube is the heat generated from the increased voltage. When handling the power supply, we noticed that the machine itself felt warmer at 30V than at 2V, and a change in temperature likely occurred in the capillary tube as voltage increased. An IR thermometer could be used to measure the change in temperature through the capillary tubes and, thus, help gauge the significance of temperature as an uncertainty. Increased temperature tends to increase ciliary movement by causing an increase in binding affinity between actin and myosin. Increased ciliary movement tends to lead to more rigorous eating habits but could also result in faster movement along the capillary tube (9).

To better examine whether *T. pyriformis* galvanotaxis can vary with voltage, a similar experiment could be conducted specifically in the voltage range of 2V to 10V. This would allow one to confirm whether increasing voltage leads to a step-like increase in *T. pyriformis* distribution, as well as provide insight into whether this phenomenon is due to the triggering of calcium-gated ion channels before potassium-gated ion channels.

Moreover, to fully confirm that *T. pyriformis* galvanotaxis occurred as a result of voltage-gated ion channels, the experiment should have been performed with calcium and potassium ion channel blockers, such as cadmium chloride and tetraethylammonium (TEA) chloride, respectively. If our theory is correct, blockage of these channels would decrease *T. pyriformis* cathodal distribution. However, the alternative result would suggest that *T. pyriformis* have intracellular signaling pathways that detect electrical stimuli and can instruct cilia to propel themselves towards the cathode.

Despite the uncertainty in cell counts and in the effects of temperature, our data suggests *that T. pyriformis* will begin to perform cathodal galvanotaxis when we apply a potential difference of approximately 4V across a capillary tube. Further increase in voltage during galvanotaxis caused the distribution of *T. pyriformis* at the cathode to remain at approximately 80%.

METHODS

T. pyriformis Growth and Maintenance

T. pyriformis used for this experiment were subcultured

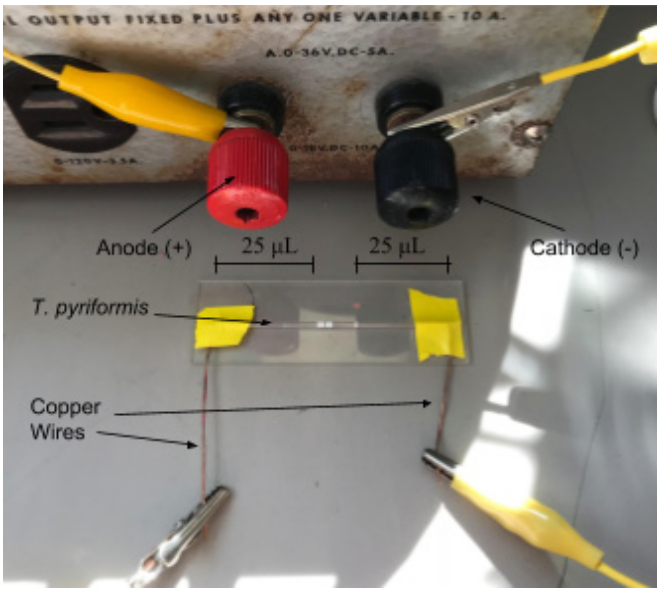

Figure 3. Experimental setup for galvanotaxis on *T. pyriformis* in an 86.5 µL micropipette capillary tube. After supplying the voltage for one minute, the anode and cathode (marked by 25 µL lines) ends of the tube were snapped off and counts of *T. pyriformis* were measured with a hemocytometer.

by adding two drops of concentrated *T. pyriformis* in axenic proteose peptone medium (Carolina Biological Supply Company) into the *Tetrahymena* subculture medium (Carolina Biological Supply Company 13-2315), after which *T. pyriformis* were grown in an incubator at 27°C for 2 days.

Experimental Apparatus Set-up

To determine the effect of voltage on the distribution of T. pyriformis, the Hampden voltage power supply was used to induce galvanotaxis while controlling current. Each 86.5 µL micropipette capillary tube used was snapped at the 25 µL end of the tube to generate a 61.5 µL capillary tube with markings for 25 µL at each end. Each capillary tube was inserted into a sterile 1 mL plastic pipette, and the pipette and tube were then filled with the *T. pyriformis* solution. While maintaining full volume in the capillary tube, the pipette was detached from the capillary tube. Copper leads were used to conduct electricity (**Figure 3**); the ends of the copper wires, approximately 4 inches long, were sanded to remove the paint layer and to allow for better conductivity. The capillary tube was then taped on a 1 inch x 3 inch glass slide, and the leads inserted into the ends of the tube were taped down, as well. Alligator clips attached the leads from the capillary tubes to the positive and negative ends of the power supply. A marker was used to indicate which end of the capillary tube was attached to the negative cathode end and the positive anode end of the voltage supply. Through preliminary testing, it was determined that one minute was sufficient for obtaining a significant difference in *T. pyriformis* distribution across the two ends of the tube. To measure distribution, the capillary tube was carefully snapped according to the 25 µL markings at each end of the tube. If the tubes were not precisely snapped or if there was an air bubble in the capillary tubes, the trial would be rerun in an effort to avoid uncertainty caused by the decreased amount of solution from the cathode or anode. The snapped pieces of the capillary tube were inserted into a pipette, and the solutions were squeezed out into two separate wells on a well plate. One drop of 1.5% iodine solution was dropped into each well to fix the *T. pyriformis*, and one drop of each mixed solution was counted on 9 mm x 9 mm x 0.1 mm hemocytometers to measure the distribution of *T. pyriformis* in the anode and cathode.

Experimental Procedure

To determine the exact voltage at which the distribution of *T. pyriformis* at the two ends of the tube were significantly different, voltage was varied at 0V, 2V, 4V, 10V, 20V, and 30V for final testing. Current was controlled at 5 amperes to avoid the uncertainty of the effects of current on *T. pyriformis* distribution. As determined by counting via a hemocytometer with a compound light microscope (100x), the cell density of *T. pyriformis* used for final testing was approximately 5.44 x 10^4 *T. pyriformis*/mL (dilution due to iodine is accounted for), and all data was collected in a single afternoon to reduce the uncertainty of increased cell density. The voltage was varied in 6 treatment groups, with 5 trials in each treatment group and 6 trials for the negative control. For the negative control, *T. pyriformis* was connected to the power supply at 0V for exactly one minute before the capillary tubes were snapped and the cell distribution at each end of the tube was measured with a hemocytometer.

Statistical Testing

The average number of *T. pyriformis* in the cathode and anode of all the runs were standardized to percentages so that statistical T-tests could be performed between the two ends of the tube to reveal the significance of a specific voltage on cell distribution across the capillary tube. Data was standardized so that the *T. pyriformis* count in cathode and anode added up to 100%; however, the anode piece and cathode piece snapped off does not account for total volume of *T. pyriformis* in the capillary tubes (**Figure 3**). T-tests were also performed between the treatment groups and the negative control to determine the significance of increased voltage on *T. pyriformis* distribution on the cathode end of the tube. Because of the large number of T-tests conducted, the Bonferroni correction was used to guard against false positives.

ACKNOWLEDGEMENTS

The authors would like to thank the Milton Academy Science Department for providing the materials and space for this research and for their endless support.

REFERENCES

1. Nuccitelli, Richard. “A Role for Endogenous Electric Fields in

Wound Healing." *Current Topics in Developmental Biology*, 2003, pp. 1–26., doi:10.1016/s0070-2153(03)58001-2.
2. Ibañez-Tallon, Inés. "To Beat or Not to Beat: Roles of Cilia in Development and Disease." *Human Molecular Genetics*, vol. 12, no. 90001, 2003, doi:10.1093/hmg/ddg061.
3. Jenkins, Paul M *et al*. "Olfactory cilia: linking sensory cilia function and human disease" *Chemical Senses*, vol. 34, no. 5, 2009, pp. 451-64.
4. Giannini, John, and Michele Severson. *Tetrahymena* Experiment Manual. St. Olaf College, 2015, pp. 1-45, pages.stolaf.edu/wp content/uploads/sites/803/2016/03/Giannini_and_Severson_Manual_on_Tetrahymena_Experiments_2015.pdf
5. Kim, Jihoon, *et al*. "Quantitative Measurement of Dynamic Flow Induced by *Tetrahymena Pyriformis* (T. Pyriformis) Using Micro-Particle Image Velocimetry." *Journal of Visualization*, vol. 14, no. 4, 2011, pp. 361–370, doi:10.1007/s12650-011-0102-1.
6. Oud, Machteld M *et al*. "Ciliopathies: Genetics in Pediatric Medicine." *Journal of Pediatric Genetics* vol. 6, no. 1, 2017, pp. 18-29. doi:10.1055/s-0036-1593841
7. Kim, Paul Seung Soo, *et al*. "Chapter 11: Magnetic Swarm Control of Microorganisms." *Microbiorobotics: Biologically Inspired Microscale Robotic Systems*, edited by MinJun Kim et al., Elsevier, 2017, pp. 221-244.
8. Reece, Jane B., and Neil A. Campbell. *Biology*. 10th ed., Pearson, 2014, pp. 1067.
9. Gangar, Surekha, Shayini Kanageswaran, Siana Lai, and Anne Persson. "Effect of temperature and time on the ciliary function of *Tetrahymena thermophila* based on food vacuole formation." *The Expedition*, vol 5, 2015.

Received: March 8, 2019
Accepted: April 24, 2019
Published: June, 2019

Financial Support: Thanks to JEI Sponsor Alloy Therapeutics for support of this article's publication.

JOURNAL OF
EMERGING INVESTIGATORS

Article

Pichia kudriavzevii yeast exposure increases the asthmatic behavior of alveolar epithelial cells *in vitro*

Valentina Ortega[1], Leya Joykutty[1]
[1]American Heritage School, Plantation, Florida

SUMMARY

Asthma is a respiratory disorder that is characterized by the obstruction of the airway due to mucus overproduction and inflammation. More than 334 million people worldwide are affected by asthma. *Pichia kudriavzevii* is a spoilage yeast that is abundant in the environment and therefore a proficient pathogen. In this study, we observed the asthmatic effects of *P. kudriavzevii* on alveolar epithelial cells through a trypan blue assay (viability), TUNEL assay (apoptosis), PAS stain (mucin presence), and an ELISA immunoassay (IL-6 hypersecretion). Results from the assays displayed a direct correlation between infection duration and asthmatic characteristics. Thus, the *P. kudriavzevii* yeast may be a common cause of asthma-related symptoms and is a worthy cause of further study.

INTRODUCTION

Asthma is a multicellular respiratory disorder that affects more than 334 million people worldwide (1). It is mainly characterized by the obstruction of the respiratory tract due to increased mucus production by the airway's epithelial cells and inflammation of its smooth muscle. It is currently believed that inhaled environmental stimuli trigger the molecular and cellular pathways that drive the clinical manifestations of asthma and other respiratory diseases (2, 3).

The major molecular and cellular indicators of asthma include elevated cytokine production, overproduction of mucus, and increased apoptosis of airway epithelial cells. Environmental stimuli trigger the production of cytokines, such as IL-25 and IL-33. These cytokines promote the production of other cytokines, such as IL-6 (4). IL-6 is known to contribute to the deterioration of the lungs and their function. A 2011 study suggested that a polymorphism in peripheral blood mononuclear cells (PBMC) was largely responsible for the magnification of several asthma-related symptoms, primarily through the induction of cytokine overproduction (5). These altered cytokine levels are also known to contribute to decreased viability of airway epithelial cells. A study identified the exfoliation of airway epithelial cells, as well as the thickening of the basement membrane of the bronchi, as crucial indicators of asthma in patients (6).

In addition to the increased production of cytokines, environmental stimuli trigger the increased production of mucus. Mucus is a viscous solution that is produced by the mucous membranes lining the epithelial surfaces of organs, such as the surfaces of airways in the lungs. Mucus is composed of antiseptic enzymes and glycoproteins. In asthma, repeated exposure to environmental stimuli promotes secretory cell hyperplasia, the overabundance of mucin-secreting goblet cells in the epithelial layer of the airway, which leads to mucus overproduction (7). Although mucus overproduction in asthma originates in the large airways (structures such as the primary bronchi that are >2mm in diameter), it also extends to the small airways (central and peripheral airways <2mm, such as the bronchioles and alveoli) as the blockages break off, continue travelling down the respiratory tract, and impair airflow and oxygen exchange in the smaller structures of the lungs (8). In addition, it is not uncommon for airway epithelial cells to apoptose as a result of asthma-related eosinophil overproduction. In fact, it is one of the crucial indicators of the disease. A study identified the exfoliation (a form of apoptosis) of airway epithelial cells, as well as the thickening of the basement membrane of the bronchi, in asthmatic patients as crucial indicators of the disease (6).

Some cytokines, including IL-25 and IL-33, are released at the moment that environmental stimuli interact with airway epithelial cells. These cytokines go on to produce other cytokines such as the one we tested in this study: IL-6 (4). IL-6 is an inflammatory marker with a key role in the development of asthma due to its fundamental contribution to the deterioration of the lungs and their function. IL-6 is present in elevated quantities within the bronchoalveolar fluid (BALF) in the lungs of asthmatic patients and upon secretion by alveolar epithelial cells, it augments asthma symptoms by inducing inflammation in the smooth muscle cells of the airway (5). Airway epithelial cell viability in asthma is also often decreased due to the elevated cytokine levels and overall respiratory system dysfunctionality. In fact, a 2011 study suggested that a studied polymorphism in peripheral blood mononuclear cells (PBMC) was largely responsible for the magnification of several asthma-related symptoms, primarily through the induction of cytokine overproduction (5). This further supports the importance of cell viability in the epithelium of asthmatic subjects and its ability to potentially indicate the occurrence of the disease within such asthma patients.

In this study, we will test the effects of *Pichia kudriavzevii* on the cell viability, apoptosis, cytokine production (IL-6), and mucus production of A549 alveolar epithelial cells. *P. kudriavzevii* is a low pH spoilage yeast and is an anamorph of *Candida krusei*. *P. kudriavzevii* can be found in the natural and commercial environments, including in fruits and their many commercial derivatives (9). Thus, this yeast can be considered easily acquirable through exposure to its

intermediate hosts. In addition, *Candida albicans,* a closely related species of *P. kudriavzevii*, has been thoroughly studied, and many studies concluded that it is a primary cause of asthma-related symptoms in asthma patients (10). Data from multiple studies have continuously suggested the opportunistic pathogenic potential of *C. albicans* in hosts with a compromised immune system. These data have especially emphasized the yeast's potential role in the development of asthma and the augmentation of preexisting asthma symptoms in affected patients (11). A foundational study on *C. albicans* also observed yeast-initiated wheal and flare reactions in approximately 58% of the tested asthma patients, thus strengthening the hypothesis that *C. albicans,* and possibly other related species, may considerably contribute to the pathophysiology of asthma in some patients (12).

Although the properties of *P. kudriavzevii* have not yet been tested on any cell lines in order to evaluate its potential effects, an ongoing *in vivo* study heavily suggests there is a connection between the yeast and asthma (13, 14). As such, the possibility exists that *P. kudriavzevii* exhibits similar properties as its anamorph *C. albicans* and is therefore responsible for the asthma-related symptoms in its affected subjects. This study thus aims to understand the molecular asthmatic effects of *P. kudriavzevii* yeast secretions on A549 alveolar epithelial cell behavior, and in doing so increase the understanding of environmental allergens and their effects on the pathogenesis of asthma. Additionally, this study aims to recognize the asthma-related effects of *P. kudriavzevii* on the airway in order to build the foundation for future research on allergen-targeted asthma treatments.

RESULTS

Alveolar epithelial cells exposed to P. kudriavzevii exhibit increased cell death

Previous literature suggests a strong correlation between increased exposure to asthmatic agents and subsequent decreased cell viability. Thus, decreased cell viability was a predicted effect of *P. kudriavzevii* infection of A549 alveolar epithelial cells. To measure the cell viability prior to and after cell exposure to the yeast, a trypan blue assay was performed. Non-viable cells were stained blue due to trypan blue's penetration of the damaged cell membranes of dead cells and were counted using the ImageJ software. Treated (experimental) and untreated (control) groups of alveolar epithelial cells were tested via the trypan blue assay at 0, 4, 6, 12, 24, and 48 hours of incubation. All infection treatment durations displayed statistically significant differences (**Figure 1**). We also saw an indirect correlation between cell viability and increased duration of infection treatment. Thus, the data from the trypan blue assay strongly supported the hypothesized, progressively worsening effects of *P. kudriavzevii* treatment on alveolar epithelial cell viability.

Alveolar epithelial cells exposed to P. kudriavzevii also exhibited increased levels of IL-6

Another major indicator of elevated asthma-related cellular events is IL-6 hypersecretion. Previous studies have established a strong correlation between elevated IL-6 concentrations and increased asthma progression (17). Thus, we tested IL-6 concentrations both prior to and after *P. kudriavzevii* infection, in order to draw conclusions regarding the effects of the yeast on asthma-related events occurring

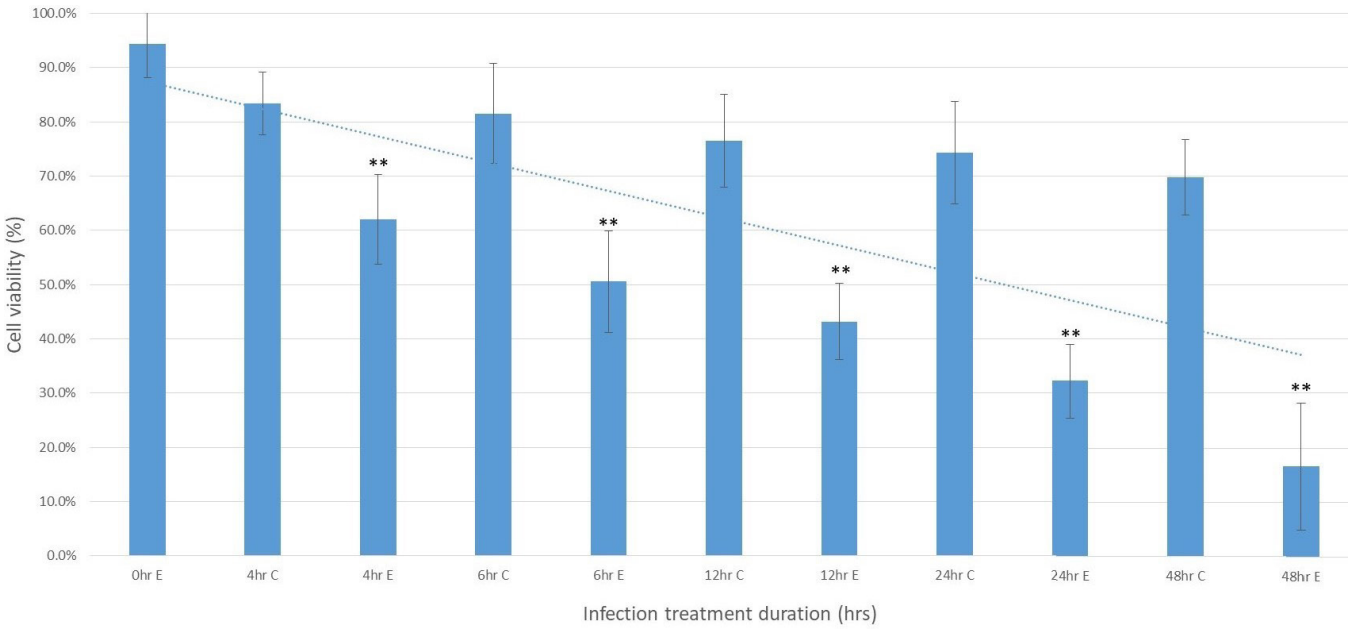

Figure 1: Cell viability as measured by trypan blue assay. Each bar represents the average cell viability within the 10 samples assayed per duration time. The letters E and C adjacent to the infection durations in the bottom legend indicate experimental infected cells and control non-infected cells, respectively. Error bars indicate 95% confidence interval, * $p<0.05$, ** $p < 0.001$.

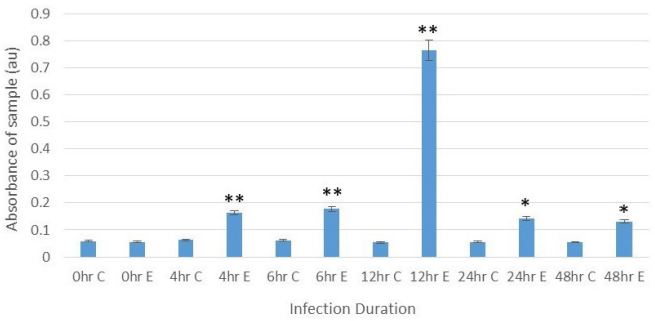

Figure 2: IL-6 concentrations in cell samples measured by ELISA. Average absorbance readings from each treatment duration were plotted against the IL-6 standard curve to obtain an approximate concentration of IL-6 present in the sample. E and C indicate experimental infected cells and control non-infected cells, respectively. Error bars indicate 95% confidence interval, *p<0.05, **p < 0.001.

in these cells. Treated (experimental) and untreated (control) groups of alveolar epithelial cells were tested via the ELISA IL-6 immunoassay at 0, 4, 6, 12, 24, and 48 hours of incubation. Every variation of the experimental infection duration was found to have significantly higher levels of IL-6 than that of the 0 hour infection (control) group (**Figure 2**). Thus, a valid conclusion is that in all the experimental groups, the *P. kudriavzevii* infection triggered the hypersecretion of IL-6, a fundamental asthmatic indicator, by the alveolar epithelial cells. However, the data also displayed results that were not statistically significant in the IL-6 concentration differences between the infection groups of 4, 6, 12, 24, and 48 hours, thus suggesting that the production of IL-6 by A549 alveolar epithelial cells peaks after only 4 hours of *Pichia kudriavzevii* stimulation (**Figure 2**).

Alveolar epithelial cells exposed to P. kudriavzevii exhibited elevated levels of polysaccharides, the primary precursor to mucus overproduction in organisms

Increased levels of polysaccharides, quantified with the PAS staining assay, is a critical indicator of asthma-related cellular symptoms and is an excellent marker of future mucus hypersecretion. As such, we performed a PAS staining assay to stain polysaccharide contents in the cell samples, and thus measured quantities of polysaccharides in A549 cells both prior to and following *P. kudriavzevii* exposure. Similar to the results from the trypan blue assay, results from the PAS staining assay showed sequentially higher concentrations of polysaccharides in the cell samples as the duration of the infection treatments increased (**Figure 3**). The control, as opposed to the experimental samples, remained constant in its low polysaccharide levels throughout the 48 hours in culture without any exposure to the *P. kudriavzevii* yeast. Thus, once again, a direct correlation between increased asthmatic indicators (in this case mucin overproduction) and increased duration of infection treatment was established.

Alveolar epithelial cells exposed to P. kurdiavzevii yeast exhibited increased levels of apoptosis in most cases

Cell apoptosis is a fundamental indicator of ongoing asthma-related events at the cellular level. Quantification of apoptotic cells in both the control and experimental samples therefore gives insight into the pathogenesis of the disease and its manifestations at the cellular level. As such, the TUNEL assay was conducted to identify cells undergoing apoptosis by staining them a dark shade of brown, which could easily be identified and quantified using the ImageJ software. The dark-stained apoptotic cells significantly increased in the infection treatment groups of greater durations, compared to those of shorter durations and the 0 hr (control) group (**Figure 4**) (student's t-test, p<0.05). Although only infection duration groups of up to 6 hours were able to be tested via this assay, we established a direct correlation between asthmatic cellular indicators (in this case apoptosis) and duration of infection treatments.

DISCUSSION

Currently, over 300 million patients worldwide reportedly suffer from asthma, and that number increases in developing countries and regions of the world where medical service is largely inaccessible (1). Successful identification of *Pichia kudriavzevii* as a biological asthmatic agent at the cellular level allows for further identification of inorganic asthmatic agents in the biosphere, such as its intermediate hosts in the natural and commercial environments. Analysis of the molecular composition of the yeast secretions responsible for the asthmatic cell behavior can lead to the identification of crucial, molecular asthmatic agents that can be targeted in novel asthma treatments and thus aid in their development. Our experiments yielded results that supported the proposed alternative hypothesis that *P. kudriavzevii* plays a role in the initiation of asthma-related symptoms and events at the cellular level. In all four of the conducted assays, the infection treatments of sequential durations all exhibited significant increases in asthmatic indicators, when compared

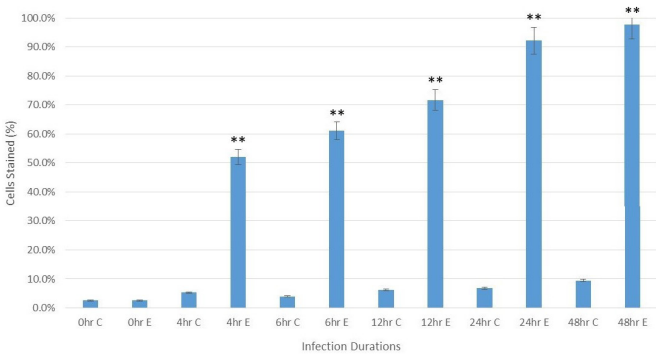

Figure 3: Mucus production by A549 alveolar epithelial cells as measured by the PAS staining assay. The bar graph displays the average results from the 10 samples in each treatment group. Error bars indicate 95% confidence interval, *p<0.05, **p < 0.001.

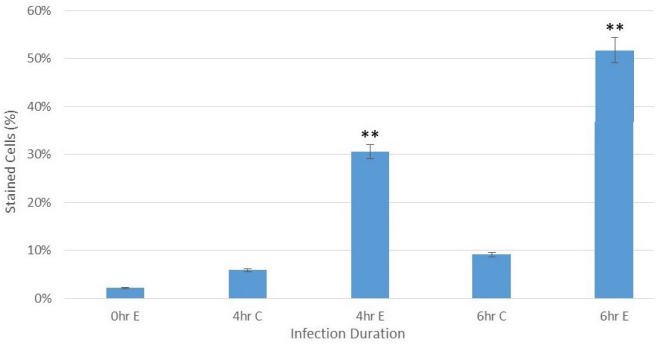

Figure 4: Apoptosis in A549 alveolar epithelial cell samples as measured by the TUNEL assay. Each bar represents the average number of apoptotic cells within the 10 samples assayed per treatment duration. Error bars indicate 95% confidence interval, $^{**}p < 0.001$.

to the control group. Furthermore, results from many of the conducted assays showed a strong direct correlation between infection duration and asthmatic cellular behavior. More specifically, we concluded that alveolar epithelial cell exposure to *P. kudriavzevii* resulted in decreased cell viability for all infection durations, increased IL-6 secretion in all infection durations, elevated polysaccharide contents in all infection durations, and significantly higher levels of apoptotic cells in the 4 hour and 6 hour infection durations. Furthermore, the effects seen in cell viability, mucus overproduction, and apoptotic cell content were all magnified as the duration of the *P. kudriavzevii* exposure increased. In contrast, IL-6 concentrations were elevated in all experimental groups, but failed to show a direct correlation with the duration of the infection, suggesting that IL-6 hypersecretion is a fundamental asthmatic indicator that is elevated after contact with the yeast yet is independent of the duration of this contact. To further support the conclusion that *P. kudriavzevii* was the initiator of these various asthmatic symptoms, uninfected control cells were grown simultaneously and assayed at the established experimental intervals along with the experimental infected cells (**Figures 1-4**). The untreated (control) groups at the various time intervals exhibited no significant asthma-related symptoms, thus suggesting that the *P. kudriavzevii* infection was the sole initiator of the asthmatic behavior in the alveolar epithelial cells.

The TUNEL assay for apoptosis was successfully conducted in infection duration groups of 0,4, and 6 hours, and the data collected provided evidence towards a direct correlation between asthmatic cellular indicators (in this case apoptosis) and duration of infection treatment. Interestingly, we could not assess apoptosis in the remaining infection durations (12, 24, and 48 hours), due to the cells' excessive detachment from the coverslips. This suggests that the *P. kudriavzvevii* yeast may have induced cell lifting at an unprecedented level in the samples with longer infection durations. In response to this observation, two new groups in-between the attaching 6-hour group and detaching 12-hour group were created to observe cell adherence both before and after exposure to *P. kudriavzevii*. The two groups had exposure durations of 8 and 10 hours, respectively. We observed significant cell detachment in the 8 hour and 10 hour groups in the post-infection condition compared to the pre-infection condition. These findings provided additional evidence for the hypothesized negative asthmatic cellular effects of the *P. kudriavzevii* yeast on alveolar epithelial cells. Improper cell attachment is a sign of upcoming apoptosis and airway remodeling, both fundamental steps in the asthmatic pathway. Induced cell lifting could indicate worsened cell function, another important characteristic of asthma. The relationships established by these data also support the direct correlation between asthmatic cellular indicators (in this case cell detachment) and duration of the infection treatment.

The next step in the expansion of this research would be to include an additional model cell line or other model organisms to further expand the perspective of the cellular asthmatic effects of *P. kudriavzevii* yeast. This expansion could give additional insight into the true asthmatic physiological effects of the yeast secretions on the two main types of cells involved in asthmatic pathways within the respiratory tract (alveolar epithelial cells and smooth muscle cells). By testing the inflammatory responses of this cell type when exposed to the yeast infection treatment, a greater understanding of the pathogenesis of asthma can be achieved. Thus, a subsequent step in the broader analysis of these asthma-related symptoms would be to conduct similar experimentation using tissue from the respiratory tract as the model of the study. By doing this, we could identify many properties that would not be otherwise involved in the individual cell line models. These properties could play a major role in the reaction to the yeast secretions and thus potentially dictate a different result with a much wider variety of implications that could augment the results exhibited in this study by the singular A549 cell line. Testing the short-term asthmatic effects of these *P. kudriavzevii* yeast secretions at an organismal level would greatly contribute to the understanding of its molecular, cellular, and physical effects on a living, functioning organism. A worthy potential model organism, and a relatively new addition to the known model organisms for asthma research, the *Drosophila melanogaster* mutant for asthma, has been used in recent studies involving the effects of gene therapy on asthma-related behavior in the cells of the airway (18).

As such, by gradually expanding the complexity of the model of study in this research, more comprehensive data can be compiled, and thus more knowledge acquired on the many different asthmatic physiological and physical effects of *P. kudriavzevii* on an organism and its many working units. Through the subsequent analysis of these results, proteins and other molecules found in the yeast secretions can be further inspected as potential asthmatic agents and therefore linked to many other microorganisms within the biosphere. The identification of additional asthmatic agents in the biosphere has immense potential to aid in the development of

more targeted asthma treatments that can combat the cellular effects of such molecules.

METHODS

Culture conditions and infection treatment

The immortalized alveolar epithelial cell line was cultured (RPMI 1640 cell culture media; supplemented with 10% FBS, penicillin, L-glutamine) until it reached the optimal confluency of approximately 85% (incubated at 37°C with 5% CO2). The *P. kudriavzevii* yeast culture (ATCC® 6258™) was cultured in YPD liquid broth media and YPD growth media agar plates (Sigma Aldrich Y1375, Y1500 respectively). After initial culturing of the necessary model cells to sufficient confluence (~85%), the experimentation was promptly started and carried out as follows: using sterile technique, the confluent alveolar epithelial cells were lifted from one of the T75 flask's surface into suspension with the use of cell scrapers, and 2ml of the created suspension was then transferred into each well of the 6-well plates being used. For every infection treatment, 10 cell culture-treated Thermanox™ coverslips were inserted per 6-well plate (2 per well; immediately before cell seeding) for optimal attachment of cells and subsequent usage in the TUNEL and PAS staining assays. The 6-well plates were incubated under A549 cell optimal growth conditions for 24-48 hours (as needed) until proper surface attachment and ~85% confluence was achieved by the cells. *Pichia* yeast were introduced to the A549 cell line through yeast culture incubation in 6-well plate inserts (pore size 0.22 µm) for 0, 4, 6, 12, 24, and 48 hours. Non-infected controls were also incubated and assayed at these time intervals for reference. After the infection treatment, both the experimental and control cell samples were assayed using the following protocols.

Trypan blue cell viability assay

Cell viability was tested via the Trypan Blue proliferation assay (15). The materials necessary to conduct the trypan blue assay for proliferation were provided by the American Heritage School laboratory facilities. To start the trypan blue staining procedure, 100 µl cell suspension was diluted in 100 µm 0.4% Trypan Blue solution, creating a 1:1 dilution which was promptly inserted into the hemocytometer for counting. Cells were counted under an inverted microscope in four 1x1 mm squares of each chamber and thus average cells per square were determined. Appropriate formula was used to determine percentage cell viability and results were analyzed in a five-number summary and through a t-test to determine significance.

ELISA to assess cytokine levels

To start the IL-6 EISA immunoassay (Enzo Life Sciences™ catalog # ADI-902-033, Cayman Chemicals™ catalog # 501030), 100 µl of base media were added into to appropriate wells in duplicates. Additionally, 100 µl of standard, sample, or control were dispensed into their appropriate wells, with the samples being taken from the liquid supernatant of the monolayer A549 cell culture. The plate was then incubated for 1 hour at room temperature in an orbital shaker at approximately 300 rpm. After the incubation, each well was aspirated and washed using the previously prepared wash buffer, repeating the process three times for a total of four washes. The provided yellow antibody (100 µl) was added to each well and the plate was then covered with a new adhesive strip and incubated for 1 hour at room temperature in an orbital shaker. The aspiration/wash process was repeated, and 100 µl of the provided blue conjugate was added to each well and the plate was then incubated for 30 minutes at room temperature in an orbital shaker at 300 rpm. The aspiration/wash process was repeated, and substrate Solution (100 µl) was added to each well (except the blank) and the plate was then incubated for 15 minutes at room temperature in an orbital shaker at 300 rpm. Immediately after incubation, 100 µl of Stop Solution 2 was added to all corresponding wells. Wells were thereafter read at 450 nm wavelength in a well-plate spectrophotometer and data was collected. The absorbance results yielded from the samples tested in the IL-6 (human) ELISA immunoassay (**Figure 2**) were plotted on a constructed IL-6 standard curve and used to derive a theoretical concentration of IL-6 in the corresponding samples (such concentration being dependent on where the collected absorbance measurement landed on the standard curve). The concentrations of IL-6 in the tested samples were analyzed using a t-test to derive statistical significance between groups.

PAS mucus secretion assay

Mucus secretion was tested via PAS (Periodic Acid Schiff) staining (16). Following manufacturer's procedures for the PAS staining assay (PolySciences, Inc™ 24200-1), stored coverslips were re-hydrated in distilled water and immersed in Periodic Acid Solution for 5 minutes, after which distilled water was used to rinse them (4 times). Coverslips were then covered in Schiff's Solution for 15 minutes, and distilled water was used to wash the coverslips. Coverslips were stained in Hematoxylin for 2-3 minutes, then rinsed in running tap water for 2-3 minutes. The pre-prepared Bluing Reagent was applied for 30 seconds and distilled water was subsequently used to rinse the coverslips. Finally, the coverslips were dehydrated using graded alcohols (100%,95%,80%,75%), and cells were viewed under an inverted light microscope. Subsequent data analysis was done using the cell counting feature on ImageJ software (NIH, 2018). The results from the PAS stain assay (Figure 3) were also analyzed in a five-number summary and by running a t-test with the raw results as to establish statistical significance of the acquired data. The conducted analysis yielded p-values of less than 0.05 when any of the experimental groups were compared to one another and to the 0 hr infection control group.

TUNEL assay to assess apoptosis

The TACS® 2 TdT DAB (TUNEL) diaminobenzidine kit (Trevigen™ 4810 30 K) was used in this experiment to

identify and quantify the number of apoptotic cells within a cell suspension sample. Prior to the commencement of this assay, cells were fixed in 3.7% buffered formaldehyde.

To label the cells, samples were placed in 1X PBS for 10 minutes at room temperature. These were then covered with 50 µl of Proteinase K Solution and incubated for 15 to 30 minutes at room temperature, and subsequently washed 2 times in deionized water for 2 minutes each. Quenching Solution was used to completely cover the coverslips for 5 minutes at room temperature, and the samples were washed by 1X PBS for 1 minute at room temperature prior to being submerged in 1X TdT Labeling Buffer for 5 minutes. A solution of Labeling Reaction Mix was created, and 50 µl of the solution was carefully dispensed on top of each coverslip. These were then incubated at 37 °C for 1 hour in a humidity chamber and immersed in 1X TdT Stop Buffer for 5 minutes at room temperature shortly after. 50 µl of Strep-HRP solution was carefully dispensed to cover each coverslip, and these were subsequently incubated for 10 minutes at 37 °C in a humidity chamber. After incubation, samples were washed twice with 1X PBS and drenched in DAB solution for 2 to 7 minutes before a final wash with deionized water.

To counterstain the samples and optimize visibility of the results, samples were immersed in deionized water for 2 minutes, and then for 5 seconds to 5 minutes in Methyl Green. The coverslips were then sequentially dipped into washes of deionized water, 70% ethanol, 95% ethanol, and 100% ethanol. Coverslips were turned upside down and left lying flat in the dark overnight to allow them to dry. Results were acquired and analyzed using light microscopy and digital cell-counting methods, respectively (dark brown-stained apoptotic cells/ green-stained non-apoptotic cells = percentage of apoptotic cells). The results of the TUNEL assay (**Figure 4**) were compiled into a multi-bar graph and analyzed through a five-number summary and a t-test to yield *p*-values and thus determine the statistical significance of the data obtained.

ACKNOWLEDGEMENTS

I would like to extend my deepest gratitude to both of my mentors, Leya Joykutty and Kepa Oyarbide, who have provided guidance and support throughout my undertaking of this study. In addition, I would like to thank American Heritage School for their laboratory facilities and partial sponsorship of this study, which would not have been brought to fruition without their support.

I would also like to thank the various institutions which gifted assays and various materials fundamental to the success of this study: Dr. Alexandra Lucas and Dr. Masdumur Rahman of Arizona State University (provided the A549 alveolar epithelial cell line), Enzo Life Sciences™ (provided IL-6 ELISA immunoassay), Cayman Chemicals™ (provided IL-6 ELISA immunoassay), PolySciences, Inc™ (provided PAS staining assay; cat no. 24200-1), and Trevigen™ (provided TUNEL assay).

Received: April 16, 2018
Accepted: April 29, 2019
Published: June 7, 2019

REFERENCES

1. "Asthma Surveillance Data." Centers for Disease Control and Prevention, 2017, www.cdc.gov/asthma/asthmadata.htm. Accessed 3 Apr. 2019
2. Erle, David J., and Dean Sheppard. "The Cell Biology of Asthma." *The Journal of Cell Biology,* vol. 205, no .5, 2014.
3. Locksley, R. "Asthma and Allergic Inflammation." *Journal of Cellular Immunology*, vol. 140, no. 6, 2010.
4. Rincon, Mercedes, and Charles G. Irvin. "Role of Il-6 in Asthma and Other Inflammatory Pulmonary Diseases." *International Journal of Biological Sciences*, vol. 8, no. 9, 2012.
5. Sackesen, C., and E. Birben. "The Effect of CD14 C159T Polymorphism on *in Vitro* IgE Synthesis and Cytokine Production by PBMC from Children with Asthma." *Allergy,* vol 68, 2011.
6. Trautmann, Alex, *et al*. "T Cells and Eosinophils Cooperate in the Induction of Bronchial Epithelial Cell Apoptosis in Asthma." *The Journal of Allergy and Clinical Immunology*, vol. 109, no. 2, 2002.
7. Rogers, Duncan F. "Physiology of Airway Mucus Secretion and Pathophysiology of Hypersecretion." *Respiratory Care*, vol. 52, no. 9, 2007.
8. Ricciardolo, Fabio L.M., *et al*. "Acid Stress in the Pathology of Asthma." *The Journal of Allergy and Clinical Immunology*, vol. 113, no. 4, 2004.
9. Chan, Giek Far, *et al*. "Genome Sequence of Pichia Kudriavzevii M12, a Potential Producer of Bioethanol and Phytase." *American Society for Microbiology*, vol. 11, no. 10, 2012.
10. Gumouski, P. "Chronic Asthma and Rhinitis Due to *Candida Albicans*, Epidermophyton, and Trichophyton." *Annals of Allergy*, vol. 59, no. 1, 1987.
11. Nobile, Clarissa J. "*Candida Albicans* Biofilms and Human Disease." *Annual Review of Microbiology*, vol.69, 2015.
12. Mathison, David A., and John H. Vaughan. "*Candida Albicans* Sensitivity and Asthma." *The Journal of Allergy and Clinical Immunology,* vol. 47, no. 2, 1971.
13. Arrieta, Marie-Claire. "Associations between Infant Fungal and Bacterial Dysbiosis and Childhood Atopic Wheeze in a Nonindustrialized Setting." *Journal of Allergy and Clinical Immunology*, vol. 142, no. 2, 2018.
14. Servick, Kelly. "Yeast in the Gut Boosts Asthma Risk." *Science Magazine*, 17 Feb. 2017.
15. *Cell Counting Protocol - Trypan Blue Exclusion Method*. triangleresearchlabs.net/wpcontent/uploads/2015/08/Trypan-Blue-Cell-Counting-Protocol.pdf.
16. *PAS (periodic Acid Schiff) Staining Protocol*. www.ihcworld.com/_protocols/special_stains/pas.htm.
17. Gabay, Cem. "Interleukin-6 and Chronic Inflammation." *Arthritis Research & Therapy*, vol.8, no. S3, 2006.

18. Roeder, Thomas, and Kerstin Isermann. "Drosophila in Asthma Research." *American Journal of Respiratory and Critical Care Medicine*, Vol. 179, No.11, 2009.

Financial Support: Thanks to JEI Sponsor Alloy Therapeutics for support of this article's publication.

Sponsorship

Editor's Circle $10,000+

ALLOY THERAPEUTICS

Patron $5,000+

NEW ENGLAND BioLabs® Inc.
enabling technologies in the life sciences

PORTFOLIOS WITH PURPOSE®

Institutional Supporters

HARVARD UNIVERSITY

HARVARD MEDICAL SCHOOL

Tufts UNIVERSITY

Charitable Contributions

We need your help to provide mentorship to young scientists everywhere.

JEI is supported by an entirely volunteer staff, and over 90% of our funds go towards providing educational experiences for students. Our costs include manuscript management fees, web hosting, creation of STEM education resources for teachers, and local outreach programs at our affiliate universities. We provide these services to students and teachers entirely free of any cost, and rely on generous benefactors to support our programs.

A donation of $30 will sponsor one student's scientific mentorship, peer review and publication, a six month scientific experience that in one student's words, 're-energized my curiosity towards science', and 'gave me confidence that I could take an idea I had and turn it into something that I could put out into the world'. **If you would like to donate to JEI, please visit https://emerginginvestigators.org/support, or contact us at questions@emerginginvestigators.org.** Thank you for supporting the next generation of scientists!

'Journal of Emerging Investigators, Inc. is a Section 501(c)(3) public charity organization (EIN: 45-2206379). Your donation to JEI is tax-deductible. '

emerginginvestigators.org